Robert R. Edelman, MD • Bettina Siewert, MD • David G. Darby, MD, PhD
Venketasen Thangaraj, BS • Anna C. Nobre, PhD • M. Marsel Mesulam, MD
Steven Warach, MD, PhD

Qualitative Mapping of Cerebral Blood Flow and Functional Localization with Echo-planar MR Imaging and Signal Targeting with Alternating Radio Frequency[1]

PURPOSE: **To create qualitative maps of cerebral blood flow (CBF) with the EPISTAR (echo-planar imaging and signal targeting with alternating radio frequency) technique.**

MATERIALS AND METHODS: **The EPISTAR technique was performed in a pig model of hypercapnia and then tested in 26 volunteers by using various paradigms for cortical activation. Echo-planar images were acquired with and without use of a radio-frequency inversion pulse applied to inflowing arterial spins. A qualitative map of CBF was then created by subtracting the image obtained without the radio-frequency pulse from that obtained with the radio-frequency pulse.**

RESULTS: **Progressively more distal portions of the tagged vessels were seen as the inflow time was lengthened until cortical enhancement was seen for inflow times of approximately 1 second or longer. Signal intensity increases from rest to sensorimotor activation ranged from 13% to 193%. CBF changes in the motor strip, primary visual cortex, and the motor area for eye movements were well localized to the cortical gray matter ribbon.**

CONCLUSION: **The EPISTAR technique is a rapid, noninvasive means for creating qualitative maps of CBF.**

Index terms: Cerebral blood vessels, flow dynamics, 17.121419 • Magnetic resonance (MR), echo planar, 17.121416 • Magnetic resonance (MR), vascular studies, 17.121416

Radiology 1994; 192:513–520

It has been hypothesized that increases in cerebrocortical blood flow are coupled to increases in neuronal activity. These increases have served as the basis for studying regional brain responses to cognitive activity (1). Positron emission tomography can reliably depict changes in cerebral blood flow (CBF) in response to sensorimotor or cognitive tasks (2,3). Because of limited spatial resolution and lack of direct anatomic information, exact localization of CBF changes is problematic. There has been great interest in the use of magnetic resonance (MR) imaging for the study of cerebral function because high-resolution anatomic information can be obtained in each subject during the same testing session, MR units are available in most hospitals, and exposure to ionizing radiation is not required. We performed this study to localize functional CBF changes with an MR imaging method that permits rapid qualitative mapping of CBF in a noninvasive manner.

Several MR imaging methods have been used to study cerebral perfusion, including (*a*) steady-state imaging after administration of diffusible tracers such as perfluorocarbons or deuterium oxide (4,5), (*b*) first-pass imaging after administration of paramagnetic compounds such as gadopentetate dimeglumine (6,7), and (*c*) spin-labeling techniques in which inflowing blood is tagged by continuous or repeated adiabatic inversion pulses and the tagged protons exchange with tissue protons to cause an alteration in tissue signal intensity (8). To date, only the first-pass imaging method has been used extensively in humans (9). With this method, relative cerebral blood volume can be determined and changes due to cognitive stimulation observed (10). However, the need for an exogenous contrast agent limits the routine use of this method for activation studies. Although the spin-labeling techniques have an intrinsic appeal because they are noninvasive, it has been difficult to scale up from rat studies because of magnetization transfer effects and because T1 relaxation occurs during the transit period as the blood moves from the tagging plane into the plane of section. A noninvasive technique for depicting brain activation by using endogenous blood oxygenation level–dependent (BOLD) contrast (11–13) has become the standard of functional MR imaging studies. With this method, activation causes an increase in signal intensity on T2*-weighted images, presumably because the increase in venous oxygen saturation associated with increased CBF causes a lengthening of the T2* of venous blood. It has been suggested, however, that much of the signal intensity changes that occur with BOLD contrast are localized to macroscopic veins, thus imprecisely localizing to cortical parenchyma (14). Furthermore, this method shows only areas of change as a response to a stimulus and is not yet suitable for mapping of resting CBF.

We implemented a noninvasive MR imaging technique, called EPISTAR (echo-planar imaging and signal targeting with alternating radio frequency), for rapid, qualitative mapping of CBF. EPISTAR combines a spin-tagging radio-frequency pulse of

[1] From the Departments of Radiology (R.R.E., B.S., S.W.) and Neurology (D.G.D., V.T., A.C.N., M.M.M.), Beth Israel Hospital and Harvard Medical School, 330 Brookline Ave, Boston, MA 02215; and the Department of Radiology, Rheinische Friedrich-Wilhelm Universität, Bonn, Germany (B.S.).
Received December 8, 1993; revision requested February 8, 1994; final revision received March 25; accepted April 11. R.R.E. supported in part by a grant from the Friends of Beth Israel Hospital and National Institutes of Health grants HL48538-01A1 and HL45180; S.W. supported in part by a grant from the Harcourt General Charitable Foundation; D.G.D. supported in part by the NH and MRC of Australia. **Address reprint requests** to R.R.E.

Abbreviations: BOLD = blood oxygenation level dependent, CBF = cerebral blood flow, EPISTAR = echo-planar imaging and signal targeting with alternating radio frequency, TI = inflow time.

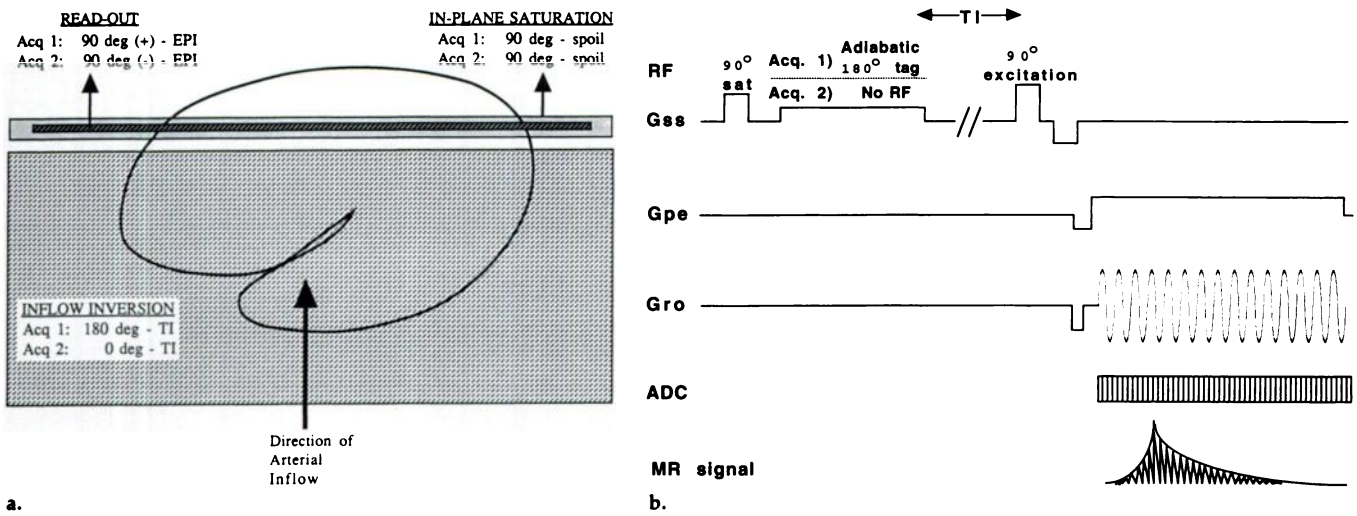

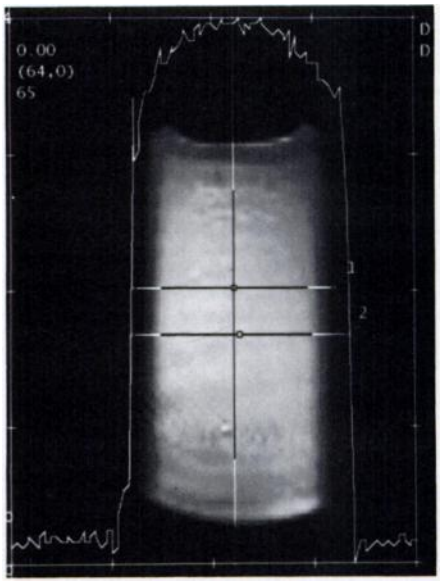

Figure 1. **(a)** Illustration of the EPISTAR technique. The 180° tagging pulse is applied during alternate acquisitions; the presaturation pulse is applied to the plane of section during each acquisition. Gradient events should be identical for all acquisitions to avoid inhomogeneities from eddy current effects. *Acq* = acquisition, *deg* = degree, *EPI* = echo-planar imaging. **(b)** Diagram of the EPISTAR pulse sequence. *Acq* = acquisition, *ADC* = analog-to-digital conversion, *Gpe* = phase-encoding gradient, *Gro* = readout gradient, *Gss* = section-selection gradient, *RF* = radio frequency, *sat* = saturation. **(c)** Profile of hyperbolic secant inversion pulse for a nominal 90-mm-thick inversion slab as measured with the EPISTAR sequence in a water phantom. The ordinate is signal intensity in arbitrary units; the abscissa is the distance in millimeters along the inverted slab. The effect of the inversion pulse is minimal at a distance of more than 50 mm from the center of the slab. Distance 1 = 90 mm, distance 2 = 100 mm.

proximal arterial blood, echo-planar readout, and image subtraction. The resulting images provide a qualitative map of CBF at various delays in the transit of blood from the proximal arterial branches to the capillaries. The basic idea is to interleave the acquisition of two echo-planar images, in one of which signal measured from blood has been reduced by the previous application of an inversion radiofrequency pulse to the inflowing spins (tagging). The tagging inversion pulse is applied proximal to the arterial supply of the cortical section being studied (Fig 1a, 1b).

MATERIALS AND METHODS

The EPISTAR sequence was performed in a pig model of hypercapnia with permission of the Animal Studies Committee. A circularly polarized head coil was used for excitation and signal reception. Sequence parameters were as follows: 5-mm-thick sections, 25-cm field of view, 128 acquisitions, and inflow times (TIs) of 800 and 1,000 msec. A 32-kg Yorkshire pig was anesthetized with intramuscular ketamine (10 mg/kg). The animal was intubated and mechanically ventilated. Anesthesia was maintained with 2% isofluorane inhalation. An arterial line was placed in the left common carotid artery for continuous pulse and blood pressure monitoring and for blood gas determinations. Hypercapnia was induced by means of ventilation with up to 70% carbon dioxide during 15-minute periods. Imaging was performed before and during hypercapnia. At the end of the study, the animal was killed with injection of a saturated solution of potassium chloride.

Twenty-six healthy volunteers were imaged according to the guidelines of the hospital committee on clinical investigations; informed consent was obtained from all subjects. Imaging was performed with a whole-body echo-planar MR imaging system at 1.5 T (Siemens Medical Systems, Erlangen, Germany). Shimming was done before imaging in all subjects. There were 128 phase-encoding steps collected during 64 msec with a bandwidth of 2 kHz per pixel; the echo was markedly asymmetric along the phase-encoding direction to shorten the echo time to 16 msec. The typical field of view was 25–32 cm, and the section thickness was 2–10 mm. A circularly polarized head coil was used for excitation and signal reception. Sequence parameters were varied for several healthy volunteers to determine the optimal technique.

A 23-msec-long hyperbolic secant inversion pulse was used with a section-select gradient of 1.3 mT/m and a nominal slab thickness of 90 mm (Fig 1c). The center of the inverted slab was positioned 60 mm caudal to the plane of section; thus, the superior edge of the inverted region was 15 mm from the center of the plane of section. A 90° radio-frequency saturation pulse with twice the thickness of the plane of section was applied to the section immediately before the inversion pulse, followed by a spoiler gradient 7 msec in duration with an amplitude of 9 mT/m. This saturation pulse eliminated potential contamination from the side lobes of the inversion pulse that might leave spurious residual signal intensity after image subtraction. Typically, 16 acquisitions (imaging time = 32 seconds for a TI of 1 second) to 96 acquisitions (imaging time = 192 seconds for a TI of 1 second) were used. The repetition time was equal to the TI. Both complex and magnitude subtractions were tested. On the basis of the initial volunteer studies, magnitude subtraction and magnitude image display were used for subsequent investigations.

Ten subjects were imaged without stimulation to study the effect of varying TI on the CBF maps. Sixteen subjects were studied at rest and while performing one of three different tasks: alternate finger tapping of one hand, full-field visual stimulation with 7.8-Hz flashing lights, or laterally alternating saccadic eye movements. A section thickness of 5 or 8 mm and a 25- or 32-cm field of view (2 × 2-mm or 2.5 × 2.5-mm pixel size) were used.

To determine the optimal TI for showing cortical activation in each subject, a series of images were obtained during rest by increasing TI by 50 msec. The TI that was 50 msec less than the one that showed

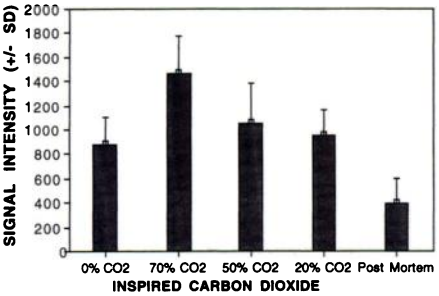

Figure 2. Chart shows signal intensity changes in a pig model of hypercapnia. The signal intensity increased with larger amounts of inspired carbon dioxide (*CO2*) and decreased after death. Residual signal intensity may be due to magnetization transfer effects. *SD* = standard deviation.

initial cortical enhancement was chosen for the activation study. EPISTAR images obtained at rest and activation were acquired at this TI, and the resulting qualitative CBF maps were subtracted to reveal a difference map. This difference map was superimposed on a high-resolution anatomic image obtained with a T1-weighted two- or three-dimensional magnetization-prepared gradient-echo sequence with rapid acquisition. After image acquisition, postprocessing involved automated coregistration of structural and EPISTAR images with AVS software (AVS, Waltham, Mass). Irregular regions of interest consisting of at least 16 pixels were drawn around the areas of activation in the subtraction image, and these regions were transposed to the original averaged images for signal intensity measurements. Measurements were also made in nearby occipital gray matter and in air outside the brain.

RESULTS

The signal intensity changes in the pig model as a response to hypercapnia are shown in Figure 2. There was a marked loss of signal intensity after death, indicating that flowing blood was the dominant contributor to image signal intensity and that magnetization transfer had only a modest effect at the long TIs used.

In the volunteers, use of a TI of at least 1 second enabled us to obtain good-quality EPISTAR images showing cortical enhancement. The signal-to-noise ratio for a TI of 1,000 msec was 30.6 ± 11.7 in gray matter (parietal cortex) and 13.6 ± 7.3 in white matter (corona radiata) (mean ± standard deviation). The cortical signal intensity as a function of TI is illustrated in Figure 3a for one subject. The portion of the vasculature shown is dependent on the TI. With a short TI (eg, 400 msec), flow was seen in major arteries. With delays on the order of 800 msec, distal branch arteries were shown. With delays of at least 1 second, the arteries disappeared and cortical enhancement was seen as the tagged blood flow entered the capillaries and tagged protons exchanged with tissue protons. In healthy subjects, the cortex enhanced uniformly with a TI of 1,400 msec or more. Cerebrospinal fluid appeared dark at all values of TI tested (Fig 3b).

In one subject, a comparison was made of EPISTAR images obtained with and without a control inversion region to cancel magnetization transfer effects. The control inversion region was 90 mm thick and was applied 60 mm cephalad to the plane of section, in alternation with the caudally positioned tagging inversion region, so that the control and tagging inversions were equal in thickness and distance from the plane of section (Fig 3c). Although the signal intensities of gray and white matter were lower with the control inversion (the latter had a signal intensity similar to that of the background), there were some drawbacks. Inferiorly draining veins were tagged and appeared on the image, and ghost artifacts occurred from pulsatile flow in the superior sagittal sinus. Although fewer veins were seen when the control inversion was not applied, veins draining cephalad from tagged regions were still observed, especially in the scalp. As a result of the direct tagging of the anterior segment of the superior sagittal sinus within the inversion slab, the posterior portion of the sinus was visualized at long TIs as the blood flowed from anterior to posterior portions. The sinus disappeared if the inversion slab was angled to avoid its anterior portion.

In the activation studies performed in volunteers, the signal intensity increases from rest to activation ranged from 13% to 193% (mean ± standard deviation, 59% ± 45). Increases were predominantly restricted to gray matter, with activity infrequently observed in subjacent white matter. For the 90-mm-thick tagging region centered 60 mm proximal to the imaging slab, a TI of 900–950 msec tended to be the optimum parameter for the cortical regions studied.

Rapid finger tapping caused an increase in signal intensity in the gray matter strip on the anterior bank of the central sulcus (Fig 4). Visual stimulation produced an increase in signal intensity in the gray matter of the calcarine cortex (Fig 5). The EPISTAR activation images were free from signal intensity changes in macroscopic cerebral veins. EPISTAR images obtained with 2 × 2-mm in-plane resolution and 2-mm-thick sections showed well-demarcated areas of increased signal intensity (increase, 117%) with visual activation. Alternating visual saccadic eye movements produced increased CBF in the cortical ribbon corresponding to the precentral gyrus motor region, which is presumed to be responsible for visual saccades (15) bilaterally in nine of nine subjects tested (Fig 6).

DISCUSSION

The EPISTAR technique is a modification of a recently described time-of-flight MR angiography technique (16), which, in turn, evolved from earlier techniques (17–19). The method provides an imaging continuum from large proximal vessels to the distal arterioles for short TIs and to the capillaries for long TIs, at which point the image represents a qualitative map of CBF. We used EPISTAR to localize CBF changes due to activation predominantly to the cortical gray matter. The precise localization of functional CBF changes to the cortical gray matter ribbon provides experimental confirmation of the main premise for the field of functional neuroimaging (ie, increases in neuronal activity cause increases in local CBF). This type of localization has the additional advantage of allowing separation of CBF changes in juxtaposed cortical regions buried within a sulcus, which is not possible with positron emission tomography. As high-resolution MR imaging improves to allow distinction of cytoarchitectonic areas, the direct mapping of CBF changes onto cytoarchitectonic areas may be possible with this technique.

Previous MR imaging methods have used exogenous tracers or spin labeling with adiabatic inversion pulses to measure CBF in a noninvasive manner. The latter method, proposed by Detre et al (8), has been successfully applied in a rat model and healthy volunteers (20). In this method, the assumption is made that the inverted spins exchange rapidly with tissue protons, causing a decrease in the signal intensity of highly perfused regions. The signal is dependent on the steady-state value of the longitudinal magnetization (M_z); after correction for T1, CBF can be quantified. Information about arterial transit time is not directly obtained. Because multiple off-resonance inversion pulses are applied, magnetization transfer effects are prominent (21). Therefore, a control image is acquired

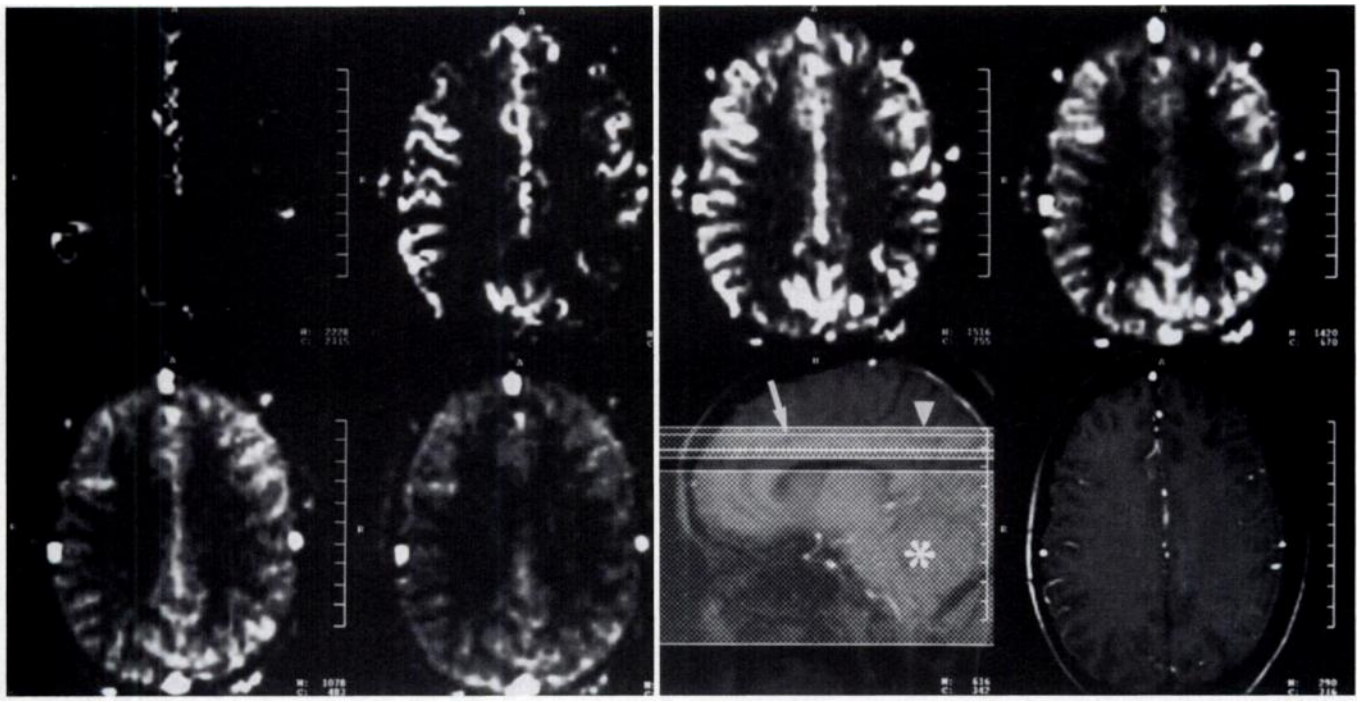

a.

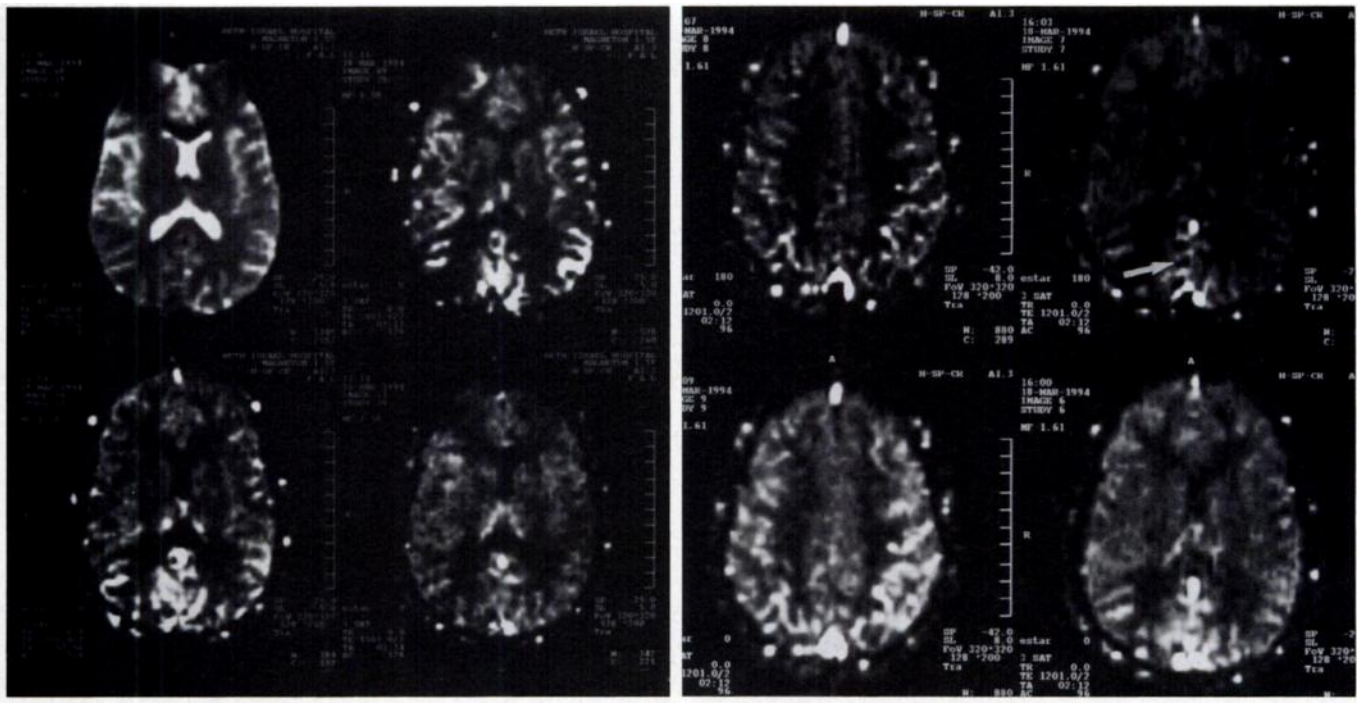

b. c.

Figure 3. Images illustrate the time course of signal intensity changes in a healthy volunteer. **(a)** EPISTAR images obtained with TIs of (from left to right and top to bottom) 200, 600, 1,000, 1,400, 1,800, and 2,200 msec. Image in the bottom row, third column is a sagittal localizer image and shows the inversion slab (*), presaturation slab (arrowhead), and plane of section (arrow). Image in lower right corner is a two-dimensional flow-compensated gradient-echo image with venous presaturation. It was obtained with the same field of view as the EPISTAR images (32 cm) and shows that the bright curvilinear structures seen on the EPISTAR images obtained with a short TI correspond to arteries. On the EPISTAR images, progressively more distal portions of the arteries are seen to enhance with increasing TI, until cortical enhancement is seen (capillary phase). **(b)** Appearance of cerebrospinal fluid. Spin-echo echo-planar image with an echo time of 100 msec (upper left) shows high-signal-intensity cerebrospinal fluid at the level of the lateral ventricles. EPISTAR images obtained with a TI of 900 (upper right), 1,200 (lower left), and 1,500 (lower right) msec show that cerebrospinal fluid has low signal intensity at all TIs. High signal intensity is seen in the choroid plexus and represents blood flow. **(c)** EPISTAR images obtained at two levels (right and left images) with (top row) and without (bottom row) a 90-mm-thick superiorly positioned control inversion region applied in alternation with the tagging inversion region, at an equal distance from the plane of section. The images are displayed at identical window settings. The control inversion reduced the signal intensities of gray and white matter; the signal intensity of the latter decreased to that of the background. Drawbacks of use of the extrainversion pulse were ghost artifacts (arrow) from pulsatile flow in the superior sagittal sinus and visualization of additional venous structures.

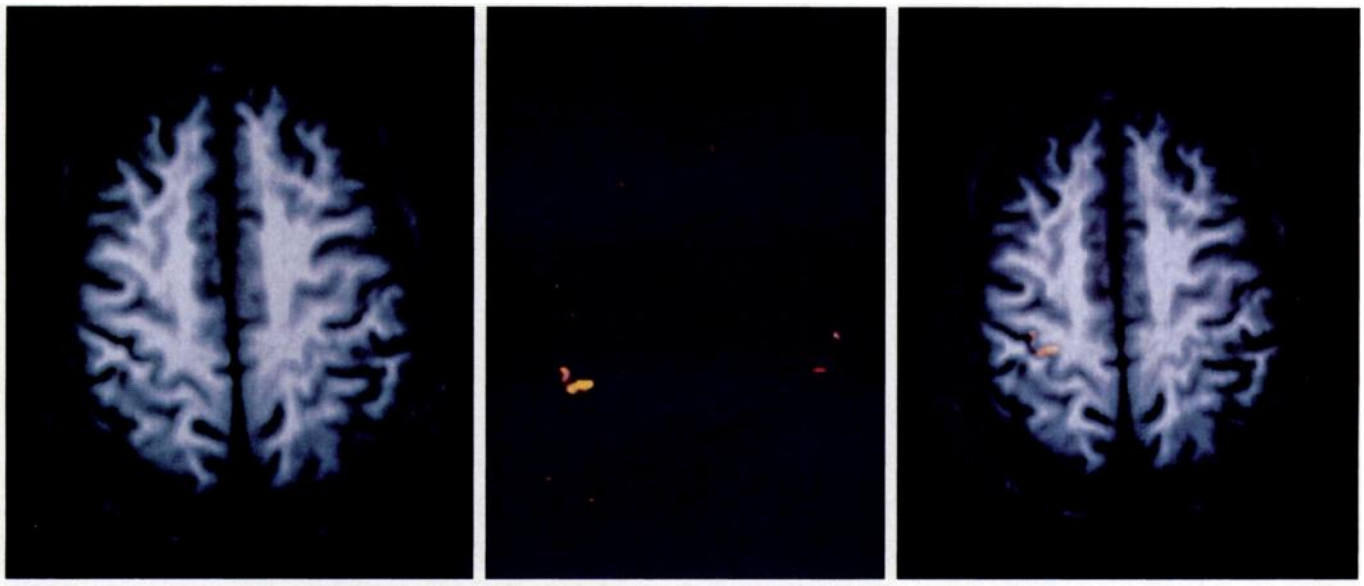

a. b. c.

Figure 4. Increased blood flow in the right motor strip with rapid alternating finger tap of left hand. **(a)** Structural image obtained with a T1-weighted inversion-recovery pulse sequence and a repetition time of 10 msec, echo time of 4 msec (10/4), TI of 500 msec, and flip angle of 15°. **(b)** Difference image of active minus rest images showing area of response. **(c)** Superimposition of difference image on structural image shows that increased blood flow maps precisely to the gray matter strip in the anterior bank of the central sulcus.

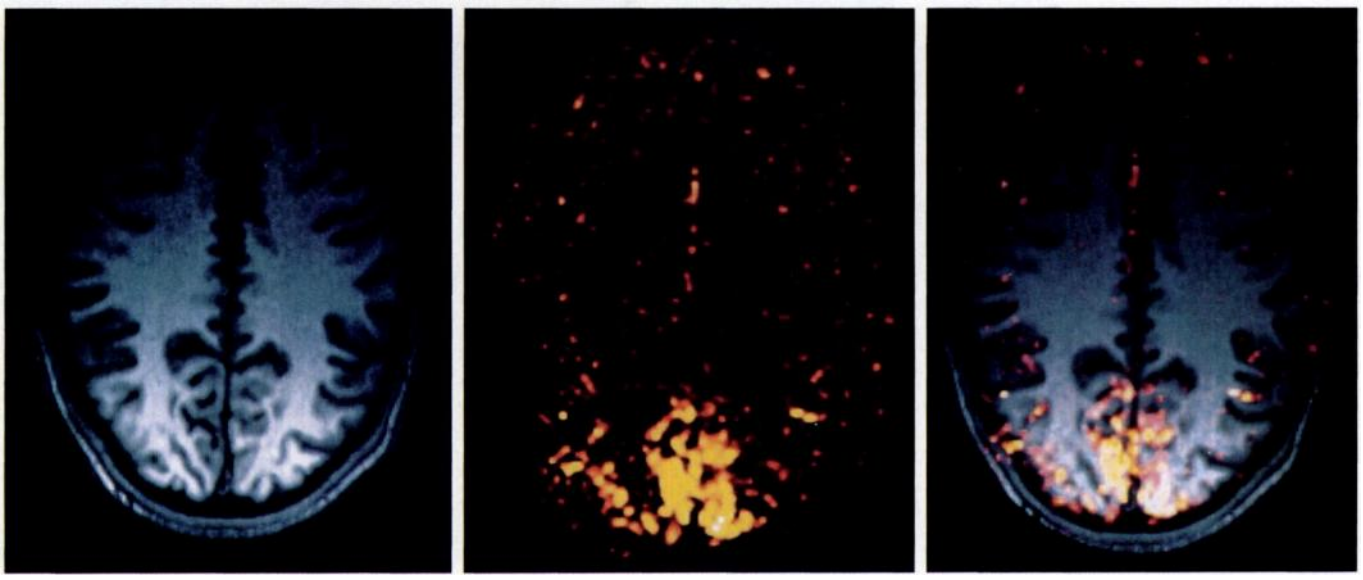

a. b. c.

Figure 5. Activation of visual cortex. Images were obtained with a circularly polarized surface coil. **(a)** T1-weighted image (10/4; TI, 500 msec; flip angle, 15°) obtained with an inversion-recovery pulse sequence for anatomic detail. **(b)** High-resolution difference image obtained with the EPISTAR technique with 4-mm-thick sections and 2 × 2-mm in-plane spatial resolution for 7.8-Hz full-field visual stimulation. **(c)** Superimposition of difference image on anatomic image. It is not certain whether the white matter activation was real or due to partial volume averaging.

in which the inversion is oppositely displaced from the plane of section compared with that used for arterial tagging. Nonetheless, imperfect image subtraction may still occur because of patient motion between acquisitions of the tagged, control, and calculated T1 images or from direct excitation of the plane of section by side lobes from the inversion pulse.

The EPISTAR sequence differs in several respects from that used by Detre et al: (*a*) With the EPISTAR technique, the magnetization transfer effects are modest because only a single inversion pulse is applied once every 2 seconds or so, versus multiple inversion pulses applied in rapid sequence with the technique of Detre et al. The magnetization transfer effects are further reduced by T1 relaxation over the long TI interval. With either technique, the magnetization transfer effects can be cancelled by the application of a control inversion region placed equidistant from the plane of section as the tagging region. Difficulties we encountered with this approach were the visualization of additional veins that were tagged by the control inversion, potentially complicating the image interpretation, and ghost artifacts from pulsatile flow in the superior sagittal sinus. However, a control inversion region may be helpful if one wishes to quantify blood flow as a function of signal intensity on EPISTAR images. (*b*) Because only a single inversion pulse is

applied, the data acquisition can be interleaved. The effects of motion are similar in the tagged and control images because of the interleaved data acquisition, so that the likelihood of image misregistration may be reduced compared with the sequential acquisition required by the method of Detre et al. (*c*) The TI, in conjunction with blood flow, determines which portion of the vasculature is depicted. With short TIs, major arteries are depicted. With TIs of less than approximately 1 second, there is little or no exchange between tagged blood and tissue protons because the blood has not yet entered the capillary bed to any substantial degree. As the TI is increased to more than 1 second, progressively greater proton exchange occurs as the tagged blood penetrates farther into the capillary bed; this proton exchange causes cortical enhancement. Images can be obtained with TIs as long as 3 seconds, the main limitation being low signal-to-noise ratios as a result of T1 relaxation of the tagged blood. Unlike Detre et al, we have not yet attempted to quantify CBF. Nonetheless, the EPISTAR images appear to provide at least a qualitative map of CBF, and arterial transit times are apparent in the time course of cortical enhancement, as shown on images obtained with various TIs. Recently, the sequence has been modified to permit true "cine" imaging with use of a reduced-flip-angle excitation and multisection and three-dimensional acquisitions.

Stimulation caused an increase in cortical signal intensity on EPISTAR images. The average increase was 59%, an order of magnitude greater than those typically found on BOLD images obtained at 1.5 T and larger than the 5%–15% change expected from CBF measurements alone (22–24). The cause of the signal intensity changes with activation are not yet known. The large change is in part an artifact of comparing subtraction images, but also relates to the choice of TI (Fig 7). The tissue signal intensity on EPISTAR images represents a summation of contributions from tagged blood protons in the capillaries at echo-planar readout and tagged protons that have exchanged from the capillaries into the tissue over the TI interval. The TI is chosen so that, at resting levels of CBF, the tagged blood just reaches the distal arteries; the capillaries are not reached to any substantial extent. As a result, there will be little cortical signal intensity on EPISTAR images. With activation, the arterial transit time is shortened so that a larger volume of tagged blood enters the capillaries well before the echo-planar readout. In this case, there is extensive exchange of tagged blood protons with cortical tissue protons. The cortical signal intensity thus becomes linked to the CBF with activation. Because the signal intensity is linked to CBF in the activated state but not in the resting state, the signal intensity changes can exceed those expected from CBF changes alone; this might not be the case if both resting and activated images were linked to CBF (eg, with the BOLD technique or that described by Detre et al [8]). Of course, this explanation is rather idealized, in that the tagged blood arrives at the capillaries not as a delta function but over a period of time.

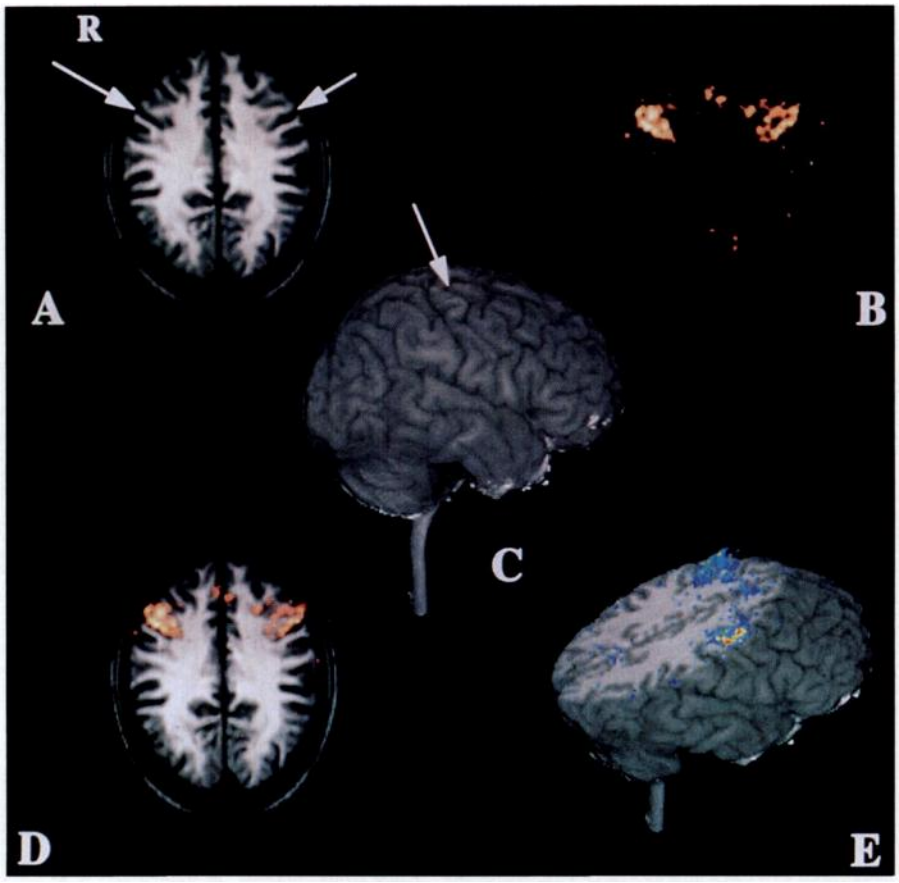

Figure 6. CBF activation during a visually guided eye-movement task. Active condition: patients were asked to look between two black boxes; a 10° visual angle separated each box from the central fixation point. Control condition: patients were asked to fixate on a cross located between the boxes. The section plane shown passed through the calcarine sulcus and the posterior junction of the superior and middle frontal gyri (55 mm superior to the plane through the anterior and posterior commissures, at an angle of −26°). The left side of the axial images corresponds to the right side of the brain. (*A*) T1-weighted image obtained with an inversion-recovery pulse sequence for anatomic detail. Arrows indicate central sulci. (*B*) EPISTAR difference image acquired with a TI of 950 msec. (*C*) Right lateral surface view from a three-dimensional reconstruction of the anatomy. Data were acquired with a three-dimensional magnetization-prepared gradient-echo pulse sequence with rapid acquisition. Arrow = central sulcus. (*D*) Superimposition of the EPISTAR difference image on the anatomic image. (*E*) Superimposition of the EPISTAR difference image on the reconstructed three-dimensional anatomic image confirms the position of the precentral gyrus activation.

Several factors determine the quality of a functional MR imaging study, including motion artifacts, venous activation, and contrast-to-noise ratio. The EPISTAR and BOLD techniques each have particular advantages and disadvantages with regard to these factors; ultimately, the two methods may prove complementary because the signal intensity changes with both techniques depend on distinct physiologic parameters. In addition to inflow effects, activation-related changes in signal intensity on BOLD images are probably caused by elevated venous deoxyhemoglobin concentrations resulting from increases in CBF. It has been suggested that these changes may be localized in medium and large superficial veins as well as in the capillary bed, making it difficult to determine the precise location of the activated cortical foci. Better local-

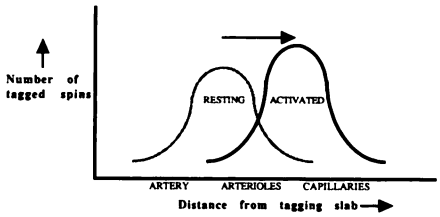

Figure 7. Illustration of the hypothesis concerning the mechanism of signal intensity changes seen at EPISTAR imaging with activation. If the TI is relatively short (eg, 950 msec), most of the tagged blood resides in the artery and arterioles, not the capillaries, at echo-planar readout. There is little exchange of tagged protons with cortical tissue protons, so that the cortical signal intensity is low and not directly related to CBF. With activation, the arterial transit time is shortened and an increased volume of tagged blood enters the capillaries, where it rapidly exchanges with cortical tissue protons. The cortical signal intensity seen on the EPISTAR image is then large and linked to CBF.

ization might be obtained by using spin-echo echo-planar BOLD imaging; however, there will be a marked loss of sensitivity. Conversely, with EPISTAR imaging, venous activation does not appear to occur. The reason is that there is nearly complete exchange of tagged blood protons with brain tissue protons during the transit through the capillary bed. Thus, most of the protons arriving in the venules are untagged and do not produce a change in signal intensity with activation; alternatively, any signal intensity changes that do occur (eg, as a result of BOLD imaging effects) will be identical for the tagged and untagged unsubtracted images and cancel with image subtraction. Given the lack of venous activation, it should be possible to localize the activated foci within the limits of the pixel dimensions (approximately 2 mm for a 25-cm field of view). In our study, activity was occasionally noted in white matter subjacent to the cortex. It is uncertain whether this activity is artifactual (eg, due to partial volume averaging) or real.

It has been suggested that at least a portion of the activity seen at functional MR imaging with the BOLD technique is an artifact of stimulus-correlated motion that results in imperfect image subtraction (25). With the BOLD technique, stimulus-sensitive cortical regions have a similarly high signal intensity on both resting and activated images. Slight subject motion between the resting and activated states then gives substantial misregistration artifacts. Brain tissue appeared dark on the rest EPISTAR image obtained with a TI on the order of 950 msec. One is subtracting a rather featureless, low-signal-intensity image from an image with much higher signal intensity in the activated regions. Given this scenario, slight patient motion should produce less severe artifacts than with the BOLD technique.

Some limitations of the EPISTAR method are also apparent. The need for image subtraction introduces sensitivity to gross patient motion, although this was not a substantial problem in cooperative subjects. The contrast-to-noise ratio appears inferior to that obtained with first-pass susceptibility contrast material–enhanced imaging, so that flow sensitivity may be less. The EPISTAR method depends on flow direction, so that an inversion region placed caudal to the plane of section would not show caudally directed flow originating cephalad to the section (eg, pial collateral vessels). Also, one must consider the orientations of the feeding vessels and the location and orientation of the plane of section when positioning the inversion region and choosing the TI. Depending on the choice of TI, signal intensity changes were occasionally seen in feeding arteries; however, these can be readily identified on a two-dimensional MR angiographic image, which can be acquired in a few seconds. Most of the signal intensity from macroscopic vessels can be eliminated by acquiring the EPISTAR images with a spin-echo echo-planar readout instead of a gradient-echo echo-planar readout. A cooperative patient and a stable MR unit with the ability to perform echo-planar imaging are essential.

In conclusion, the EPISTAR method has been validated as a noninvasive method for qualitative mapping of CBF. We showed, with use of three separate paradigms of sensorimotor activation, that CBF increases were located in the cortical ribbon of the motor cortex, the visual cortex, and the motor areas for eye movements. The EPISTAR method could prove to be a useful means for depicting CBF abnormalities in a variety of cerebrovascular disorders. ■

Acknowledgments: We thank Richard Buxton, PhD, and Robert Weisskopf, PhD, for helpful discussions.

References

1. Raichle ME, Grubb RL, Gado MH, Eichling JO, Ter-Pogossian EM. Correlation between regional cerebral blood flow and oxidative metabolism: in vivo studies in man. Arch Neurol 1976; 33:523–526.
2. Phelps ME, Mazziotta JC. Positron emission tomography: human brain function and biochemistry. Science 1985; 228:799–809.
3. Posner MI, Petersen SE, Fox PT, Raichle ME. Localization of cognitive operations in the human brain. Science 1988; 240: 1627–1631.
4. Neil JJ. The validation of freely diffusible tracer methods with nuclear magnetic resonance detection for measurement of blood flow. Magn Reson Med 1991; 19:299–304.
5. Ackerman JJH, Ewy CS, Becker NN, Shalwitz RA. Deuterium nuclear magnetic resonance measurements of blood flow and tissue perfusion employing 2H20 as a freely diffusible tracer. Proc Natl Acad Sci 1987; 84:4099–4102.
6. Belliveau JW, Rosen BR, Kantor HL, et al. Functional cerebral imaging by susceptibility-contrast NMR. Magn Reson Med 1990; 14:538–546.
7. Rosen BR, Belliveau JW, Chien D. Perfusion imaging by nuclear magnetic resonance. Magn Reson Q 1989; 5:263–281.
8. Detre JA, Leigh JS, Williams DS, Koretsky AP. Perfusion imaging. Magn Reson Med 1992; 23:37–45.
9. Edelman RR, Mattle HP, Atkinson DJ, et al. Cerebral blood flow: assessment with dynamic contrast-enhanced T2*-weighted MR imaging at 1.5 T. Radiology 1990; 176: 211–220.
10. Belliveau JW, Kennedy DN Jr, Mckinstry RC, et al. Functional mapping of the human visual cortex by magnetic resonance imaging. Science 1991; 254:716–719.
11. Ogawa S, Tank DW, Menon R, et al. Intrinsic signal changes accompanying sensory stimulation: functional brain mapping with magnetic resonance imaging. Proc Natl Acad Sci USA 1992; 89:5951–5955.
12. Kwong KK, Belliveau JW, Chesler DA, et al. Dynamic magnetic resonance imaging of human brain activity during primary sensory stimulation. Proc Natl Acad Sci USA 1992; 89:5675–5679.
13. Bandettini PA, Wong EC, Hinks RS, Tikofsky RS, Hyde JS. Time-course echo-planar imaging of human brain function during task activation. Magn Reson Med 1992; 25:390–397.
14. Hajnal JV, Oatridge A, Schwieso J, Cowan FM, Young IR, Bydder GM. Cautionary remarks on the role of veins in the variability of functional imaging experiments (abstr). In: Proceedings of the Society of Magnetic Resonance in Medicine 1993. Berkeley, Calif: Society of Magnetic Resonance in Medicine, 1993; 166.
15. Fox PT, Fox JM, Raichle ME, Burde RM. The role of cerebral cortex in the generation of voluntary saccades: a positron emission tomography study. J Neurophysiol 1985; 54:348–369.
16. Edelman RR, Siewert B, Adamis M, Gaa J, Laub G, Wielopolski P. Signal targeting with alternating radiofrequency (STAR) sequences: application to MR angiography. Magn Reson Med 1994; 31:233–238.
17. Sardashti M, Schwartzberg DG, Stomp GP, Dixon WT. Spin-labeling angiography of the carotids by presaturation and simplified adiabatic inversion. Magn Reson Med 1990; 15:192–200.
18. Dixon WT, Du LN, Faul DD, Gado M, Rossnick S. Projection angiograms of blood labeled by adiabatic fast passage. Magn Reson Med 1986; 3:454–462.
19. Wang SJ, Nishimura DG, Macovski A. Fast angiography using selective inversion recovery. Magn Reson Med 1992; 23:109–121.
20. Roberts DA, Detre JA, Bolinger L, Insko EK, Leigh JS. Quantitative magnetic reso-

nance imaging of human brain perfusion at 1.5 T using steady-state inversion of arterial water. Proc Natl Acad Sci 1994; 91:33–37.
21. Wolff SD, Balaban RS. Magnetization transfer contrast (MTC) and tissue water proton relaxation in vivo. Magn Reson Med 1988; 10:135–144.
22. Gur RC, Gur RE, Obrist WD, et al. Sex and handedness in cerebral blood flow during rest and cognitive activity. Science 1982; 217:659–661.
23. Gur RC, Gur RE, Obrist WD, Skolnick BE, Reivich M. Age and regional cerebral blood flow at rest and during cognitive activity. Arch Gen Psychiatry 1987; 44:617–621.
24. Lagrèze HL, Hartmann A. Data analysis in behavioral cerebral blood flow activation studies using xenon-133 clearance. Stroke 1993; 24:387–391.
25. Hajnal JV, Myers R, Oatridge A, Bydder GM, Young IR. Evidence for stimulus-correlated motion in functional neuroimaging experiments. (abstr). JMRI 1994; 4(P):60.